Afyon Kocatepe Üniversitesi Fen ve Mühendislik Bilimleri Dergisi
Afyon Kocatepe University – Journal of Science and Engineering
https://dergipark.org.tr/tr/pub/akufemubid

Araştırma Makalesi / Research Article
DOI: https://doi.org/10.35414/akufemubid.1400218
AKÜ FEMÜBİD **24** (2024) 037201 (749-757)
AKU J. Sci. Eng. **24** (2024) 037201 (749-757)

Designing a Cost-Efficient Belt-Driven 3D-Printed Syringe Pump

Makale Bilgisi / Article Info
Alındı/Received: 04.12.2023
Kabul/Accepted: 08.05.2024
Yayımlandı/Published: 27.06.2024

Düşük Maliyetli ve Kayış Aktarmalı 3B Baskılı Şırınga Pompası Tasarımı

İsmail AĞIR*

İstanbul Medeniyet Üniversitesi, Mühendislik ve Doğa Bilimleri Fakültesi, Biyomühendislik Bölümü, İstanbul, Türkiye

Öz

Biyoteknoloji, biyomedikal ve biyomühendislik gibi araştırma alanlarında, sıvıların hassas bir şekilde transferi ve kontrolü temel bir gerekliliktir. Bu amaçla çeşitli pompa ve akışkan kontrol sistemleri laboratuvarlarda kullanılmaktadır. Biyolojik sıvılarla çalışmaya uygunluğu nedeniyle şırınga pompaları daha çok tercih edilmektedir. Mevcut ticari şırınga pompalar, yüksek maliyetleri ve isteğe bağlı olarak yazılım veya fiziksel modifikasyonlar yapmanın zor olması dezavantajlarına sahiptir. Araştırmacılar bu nedenle, üç boyutlu yazıcı teknolojisi ve açık kaynak elektronik imkanlarını kullanarak kendi pompalarını tasarlayıp kullanmaya başlamıştır. Geliştirilen bu özelleştirilmiş pompalarda yaygın olarak doğrusal sürücü ve metal vidalı miller kullanılmaktadır, bu bileşenler pahalıdır ve bu yöntemle üretilen cihazların ağırlığı artmaktadır. Ayrıca bu yöntemde, milin hatveleri arasındaki oynama payından kaynaklı olarak geri tepme hatası oluşabilmekte ve bu da hassaslığı etkilemektedir. Bu çalışmada, kayış aktarma yöntemine dayanan ve metal parça kullanımının en aza indirildiği bir üç boyutlu şırınga pompası tasarlanmış; düşük maliyetli ve daha hafif bir şırınga pompası tasarımı gösterilmiştir. Geliştirdiğimiz pompa 10 mikrolitrenin altında hassaslığa sahiptir, ağırlığı 250 gramın altındadır ve maliyeti düşüktür (<41$). Çalışmamız sonucunda kısıtlı şartlara sahip olunan durumlarda, dışarıya en az bağımlılıkla üç boyutlu şırınga pompası üretme hedefine katkıda bulunulmuştur.

Anahtar Kelimeler: *Şırınga Pompası; 3B Baskı; Mikroakışkan; Pompa Tasarımı.*

Abstract

In biotechnology, biomedicine, and bioengineering research, precise liquid transfer and control are essential. Laboratories depend on diverse pumps and fluid control systems, with syringe pumps emerging as a preferred option due to their compatibility with biological fluids. Due to the high cost and limited customization options in existing commercial syringe pumps, researchers have begun designing their own custom devices, utilizing the expanding 3D printing technology and open-source electronics. Nevertheless, 3D-printed pumps often integrate metal components such as lead screws and rods to create linear drives, leading to heightened costs and increased overall weight. Furthermore, lead screws can introduce backlash errors, affecting precision due to play between the threads of the nut. In this study, a 3D-printed syringe pump design is introduced based on the belt drive method, with a focus on minimizing the incorporation of metal components. Not only is cost reduction achieved by new design, but it also results in a lighter syringe pump while minimizing backlash errors. A sensitivity below 10 microliters, a cost of less than $41, and a weight under 250 grams were achieved by the newly designed pump. The effort to develop a 3D-printed custom syringe pump, which reduces reliance on external sources, particularly in constrained environments, is strengthened by the reduction of dependency on metal parts and the increased utilization of 3D printed components.

Keywords: *Syringe Pump; 3D- Printing; Microfluidics; Pump Design*

1. Introduction

Fluid control is a critical task in many bio-related science methods, with implications for everything from drug discovery to basic research (Ozer et al. 2022, Kashaninejad and Nguyen 2023). Biofluids, which generally contain complex molecules such as proteins and cells, must be handled gently during transfer. Peristaltic and syringe pumps (also known as infusion pumps) are two of the most common types of fluid transfer devices used in biofluidic systems due to their advantages of low shear stress and easy sterilization (Lake et al. 2017, Samokhin 2020, Gucluer 2023).

Syringe pumps are essential tools in biomedical research, used to deliver precise and controlled doses of fluids in a wide range of laboratory applications, including biochemistry, chemistry, agriculture, and bioprocess studies. The general mechanism of a syringe pump consists of a linear movement mechanism driven by a motor, a syringe (plunger, barrel, and needle), and tubes.

Sorumlu Yazar/Corresponding Author: İsmail AĞIR *e-posta/e-mail: ismail.agir@medeniyet.edu.tr*

While commercial syringe pumps are readily available, their typical cost exceeds $100, posing a financial challenge. Also, they provide limited options for both mechanical and software modifications, making them less adaptable to the specific needs of specialized experiments. On the flip side, customized syringe pumps can be designed using basic electromechanical components, open-source software, and 3D-printed parts to meet the specific needs of researchers, even in challenging experimental settings (Juarez et al. 2016, Booeshaghi et al. 2019, Rogosic et al. 2022).

Additive manufacturing (AM), a transformative digital production technology, leverages computer-based modeling to enable the creation and virtual simulation of engineering designs before their rapid fabrication using 3D printing techniques like selective laser melting (SLM) and fused filament fabrication (FFF). This technology unlocks a vast array of material options, empowering the design and production of application-specific parts and prototypes with flexibility (Beaman et al. 2020, Ergene 2022, Ergene and Bolat 2022, Bolat et al. 2023, Ergene et al. 2023).

3D-printed syringe pumps offer several advantages over commercial counterparts, including lower cost, the ability to handle a wide range of flow rates, and compatibility with various biofluids, such as high-viscosity fluids and composites like clay. They can also operate at controlled temperatures and deliver unconventional fluids, such as acidic, corrosive, or highly reactive substances, by selecting printing materials and adjusting the conditions around the fluid path (Pusch et al. 2018). Additionally, 3D-printed syringe pumps can be programmed via any smart device, such as a smartphone, and controlled using the Internet of Things (IoT) to deliver fluids in complex patterns, such as combined continuous flow, pulsed flow, and ramped flow (Klar et al. 2019, Darling and Smith 2021, Tashman et al. 2022).

In this study, we introduce the design of a cost-effective 3D-printed syringe pump, named 'BD3DSP' (belt-driven 3D syringe pump), which incorporates minimal metal components. The BD3DSP is designed to be modular, allowing easy adjustments to accommodate any syringe size and making it a versatile tool suitable for a broad spectrum of applications. Considering that the BD3DSP is predominantly composed of 3D-printed components, including a 3D-printed linear rail, it can be produced in environments with constrained resources, such as emergency situations, low-budget laboratories, and remote locations like space and polar research stations. Moreover, the pump is lightweight, portable, and readily mountable on various machine hosts, including 3D printers, 2D plotters, 5-axis robotic arms, or microfluidic setups, facilitated by its universal connector plate.

2. Materials and Methods

According to a standard definition, a syringe pump typically comprises a syringe containing the fluid for transfer, a linear driver responsible for pushing the syringe plunger into the barrel, and two locking apparatuses: one for the barrel and the other for the plunger flange. In line with this concept, we developed a novel pump that integrates a 3D-printed linear rail, belt drive, and syringe holder seamlessly within a 3D-printed plate (base.stl) using Autodesk Inventor 2023 software. All part names and functions are detailed in Table 1, which can be accessed on our online repository at http://github.com/ismailagir/BD3DSP.

Table 1. Names and functions of 3D printed (STL) parts

Name	Function	Weight (g)
Base[a]	Bottom plate for mounting all other parts and the step motor.	92
Slot[a]	Provides a linear tunnel-like rail for the carrier.	76
Linear car, ha1, beltfixer	The linear rail carrier is where the belt end terminations are secured, with four bearing wheels mounted.	11
Ctight, Stight	Belt tensioning mechanism driven by a screw.	9
Tower	Connects the Splate to the base plate.	7
Splate	Bottom plate for securing the syringe components.	13
Sfront[a], Sbracket[a], Sframe[a]	Attach the syringe to the Splate.	14

[a];Components indicated with ([a]) in Table 1 were designed to be easily customizable through parametric dimension adjustments. This design feature enables the replication of the pump to accommodate various types of syringes in future studies.

In Figure 1, we presented all 3D printed components of the assembled pump. All components were 3D printed using Creality Ender 3 Pro and Tough PLA filament (Porima Inc, Turkey), with specifications detailed in Table 2.

The 3D printing was carried out with parameters set to 100% infill, a layer height of 0.2 mm, and a printing speed of 60 mm/s at 220°C, as key parameters provided in Table 3.

Table 2. Properties of the preferred PLA filament.

Property	Value
Diameter	1.75 mm
Color	RAL 7046
Density	1.22 g/cm^3 (ISO 1183)
Tensile strength	50 MPa (ISO 1183)
Elastic modulus	2400 MPa (ISO 527)
Heat deflection temperature	58°C (ASTM D648)
Glass transition temperature	55-65°C (ASTM D3418)

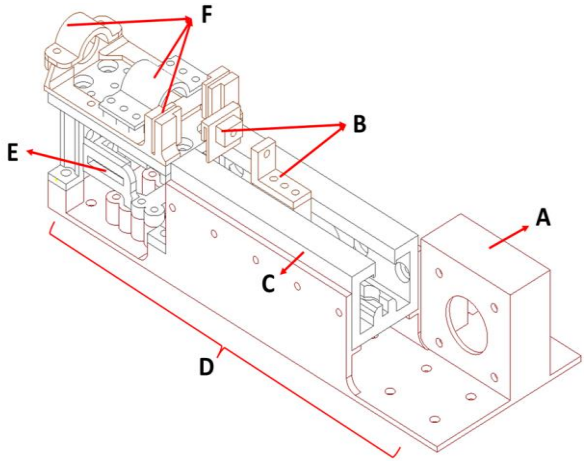

Figure 1.) Step motor mounting frame. B) Syringe plunger fixer over the sliding carriage. C) Linear rail. D) Base plate. E) Belt tensioner. F) Syringe holder.

Table 3. Key parameters of 3D printing process.

Property	Value
Bed temperature	60°C
Nozzle temperature	220°C
Fill pattern	Grid
Perimeters at vertical shells	3
Solid layers at horizontal shells	4
Print speed	60 mm/s
First layer speed	30 mm/s
Travel speed	150 mm/s
Support overhang threshold	45°
Support style	Grid
Support interface spacing	0.2 mm

2.1. Design of The Base Plate

We designed the base plate to securely hold all the components in place and to operate the stepper motor. As depicted in Figure 1-D**,** the base plate measured 220 mm in length, 60 mm in height, and 50 mm in width, with a weight of 92 grams. M4-sized holes were incorporated for the attachment of the belt tensioner and other components using M4 bolt-screws. Also, we placed 4 mm holes at the back of the plate, spaced 20 mm center-to-center, to easily integrate the syringe pump to common 20x20 aluminum profiles for various applications.

2.2. Linear Mechanism

The linear rail, or linear guide, serves the purpose of enabling smooth and accurate movement along a single axis. There are two common types of linear mechanism: lead screws and belt drives, with the key differences between these two illustrated in Table 4. Belt drives are commonly used in applications where cost, noise levels, and maintenance are prioritized, such as pick-and-place machines and packaging machinery. In contrast, lead screws are frequently employed in applications where load capacity is a primary concern, notably in CNC machines and machine tools (Schreiber et al. 2020, Khalid et al. 2023).

Table 4. Comparing properties of timing belts and lead screws.

Factor	Timing Belt	Lead Screw
Cost	Lower	Higher
Load capacity	Lower	Higher
Noise level	Lower	Higher
Maintenance	Less	More
Materials	Plastic	Metal

The lead screw enables linear movement by propelling a nut along the screw. Nevertheless, the existence of a gap between the nut and screw can introduce vibrations, potentially leading to backlash issues that may compromise the precision of controlling the movement of the syringe plunger in the pump. To improve precision and eliminate backlash, one option is to invest in precision lead screws, albeit at a higher cost. However, a more efficient alternative is to utilize ball screws, which minimize friction by incorporating small rotating balls within the nut; unfortunately, they are notably more expensive. In contrast, in a well-calibrated belt drive system, theoretically, there should be no backlash. Therefore, when designing a syringe pump with relatively small torque, opting for a belt drive would be more advantageous (Luo et al. 2022, Wang et al. 2023). Also, according to a recent study, maintenance through greasing is crucial for achieving precision in a lead screw-based pump (Leuthner and Hayden 2023). Conversely, the belt drive only requires belt tensioning and simple cleaning over time.

In 3D printing, both belt drives and lead screws are commonly employed. However, belt drives hold

particular significance due to their cost-effectiveness, capacity to enhance print speed while maintaining precision, and ease of reproducibility. In contrast, lead screws are typically designated for the Z-axis, benefitting from gravity's assistance in mitigating backlash issues, and where their higher load capacity and torque are crucial (Liu et al. 2019, Mapley et al. 2020).

Typically, a linear driver system includes components such as a slider carriage and extruded *aluminum* profiles (V-slot or T-slot). When designing a 3D-printed syringe pump, this requirement increases design costs and adds extra weight, potentially limiting customization options. As shown in Figure 2, to overcome these challenges, we fabricated a 3D-printed sliding carriage and a linear rail (slot), promoting complete in-house production. We designed the carriage with four bearings attached to slide along the rail. It is possible to use either plastic 3D printed or commercially available metal bearings (coded as 608ZZ) with specifications of a 22 mm outer diameter, 8 mm inner diameter, and 7 mm thickness. On the top of the sliding carriage, we added three M4-sized holes to attach the syringe plunger fixer, which moves the plunger according to the carriage's position.

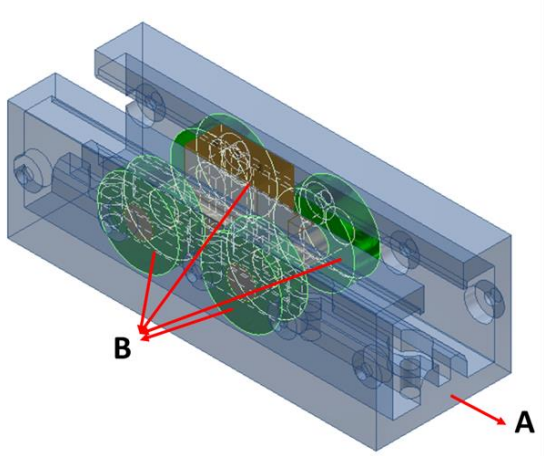

Figure 2. A) Linear rail. B) The sliding carriage and 4 bearings on the sides.

2.3. Belt Drive

GT2 (Gates Tooth 2) is a standardized code for a belt with rounded tooth profiles, signifying that the teeth are spaced 2 mm apart (Shah et al. 2019). As illustrated in Figure 3, we employed a 40 cm length, 6 mm wide GT2 rubber timing belt (Wang et al. 2018). Two 20-tooth, 16 mm diameter belt pulleys (with a 5 mm bore) are utilized, with one serving as the driver pulley mounted on the stepper motor, and the other serving as the driven pulley. This configuration creates a synchronous belt drive with a 1:1 gear ratio. At the opposite side of the belt, we integrated a belt tensioner mechanism, utilizing an M4 screw and a wing bolt. The tensioner was designed to horizontally stretch (X-axis) the belt by 5 mm and was secured in place with an additional M4 screw-bolt positioned perpendicular (Y-axis) to it. We adjusted the wing bolt to ensure the belt maintained adequate tension.

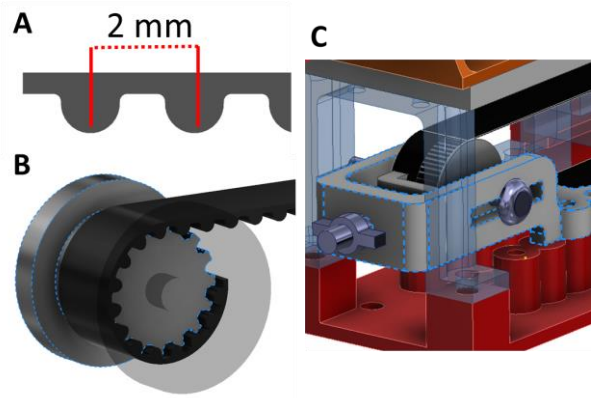

Figure 3. A) GT-2 belt. B) Belt and pulley system. C) Belt tensioner mechanism.

2.4. Operation and G-code

Step motor drivers can be directly controlled using the popular Arduino Uno board through drivers or with (CNC) shields, facilitating the setup of a control system. In CNC systems, all mechanical control is executed through the utilization of G-codes, which adhere to universal standards (RS-274).

We flashed the open-source CNC control firmware Grbl (v0.9) onto the Arduino Uno to enable the operation of the entire hardware. Since we required a single linear axis of movement, we employed a standard Nema 17 stepper motor (model 17HS4401S) with 200 steps per revolution and a holding torque of 3.2 kg-cm. For driving the stepper motor, we employed the A4988 stepper motor driver through the CNC Shield V3 (Barik et al. 2023). As the power supply, we used a 12V, 2A AC-to-DC adapter. The A4988 driver's current limit adjusted to 1.5 A, which corresponds to a Vref of 1.2 V using a multimeter. The highest linear force that the stepper can apply to the syringe piston can be calculated from the torque value provided by the factory. Assuming a pulley diameter of 16 mm based on Equation 1, the linear force is determined as 39.25 N.

$$F = \frac{Stepper\ Torque}{Pulley\ Radius} = \frac{0.314\ Nm}{0.008\ m} \quad (1)$$

$$F = 39.25\ \text{N}$$

The theoretical value of 32.25 N is then employed in Equation 2 to determine the maximum pressure within the pump. This calculation results in a pressure of 347 kPa in a system utilizing a syringe equipped with a 12 mm diameter cross-section piston.

$$P = \frac{Linear\ Force}{Cross - Section\ Area} = \frac{39.25\ N}{\pi\ *\ (0.006\ m)^2} \quad (2)$$

$$P = 374\ kPa \quad (2)$$

However, it's worth noting that the torque exerted by stepper motors fluctuates with their speed, with higher torques typically observed at lower speeds (Kukla et al. 2016). Additionally, it is necessary to adjust the operating parameters of the stepper motor to ensure that it remains continuously open after pumping, thereby maintaining its torque against potential counter pressures.

Using the G-codes in Table 5, we managed to perform several tasks, such as setting the dosage volume and flow rate, and creating flow injection cycles by inserting time breaks. When a new line of G-code is sent over UART, the machine (Grbl firmware) parses the command and then executes it. Once the command has been executed, it responds with an 'OK' message to indicate successful processing. Any smart device with UART support can be used to access and control our syringe pump. To make the pump easier to control, we created a user interface using Microsoft Visual Studio 2022 and wrote a Python script using the widely used PySerial library.

2.5. Calibration

Microstepping is a technique employed in stepper motor control, allows for finer movement resolution by breaking down each full step into smaller, incremental steps (Tashman et al. 2022). According to Equation (3), setting the microstepping to 1/16 will provide a movement precision of 1/80 millimeter, or 80 steps per millimeter. We configured the A4988 driver to operate in 1/16 step mode, which is also the default setting for the TMC2208 used in stock Ender 3 printers. The calculated steps-per-unit parameter was set using the “M92 X80.0” G-code command.

On the other hand, despite employing microstepping, additional calibration may be necessary due to slight deviations arising from imperfections in stock components like the stepper motor, belt, or pulleys. For calibration, we affixed a digital compass to the rear of the base plate and executed the "G1" g-code to move it 0.1 mm, measuring the movement with the compass in 30 iterations. Consequently, as a minimum limit, we observed a guaranteed precision of 0.1 mm with no random errors.

Table 5. Operational G-code commands and their functions.

Code	Function	Example usage
M25	Pause the process	M25
M0	Pause the process without saving the state	M0
G1 X(P)	Move to the position P	G0 X0.1; moves the syringe plunger 0.1mm
G1 F(N) X(P)	Move to the position P with the travel speed N	G1 F50 X1; moves the syringe plunger 1 mm with 50mm/s speed.
G4 P(MS)	Pause the process for the specified number of milliseconds (MS).	G4 P5000; pause the flow for 5 seconds.
$1	Idle lock time for steppers	$1=255 ; to remain continuously open

$$\frac{Steps}{mm} = \frac{Steps\ Per\ Rev.x\ \ Microstepping}{Pulley\ Tooth\ x\ Belt\ Pitch} \quad (3)$$

$$\frac{Steps}{mm} = \frac{200\ x\ 16}{20\ x2} = 80$$

3. Results and Discussion

3.1. Validating the Analytical Performance

We used a 5-milliliter polyethylene (PE) syringe with a 12-millimeter inner diameter, filling it with distilled water. As illustrated in Figure 4, for evaluating the pump's sensitivity, we used a laboratory scale to dispense distilled water into a beaker and measured the weight. We adjusted the plunger in increments of 0.1, 0.2, 0.3, 0.5, and 1 millimeter, corresponding to dispensed volumes of 11.3, 22.6, 33.9, 56.5, and 113 microliters, respectively (for a 5 mL syringe). To compensate for the scale's sensitivity, we replicated the 0.1-millimeter step five times.

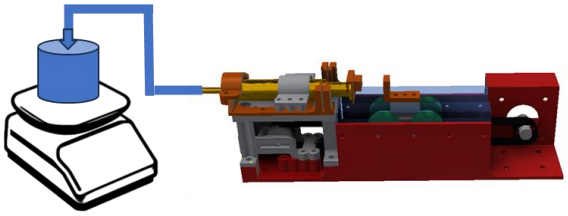

Figure 4. Setup for validating analytical performance of the pump.

Subsequently, as presented in Table 6, we evaluated the standard deviations for all steps using the measured average weight gain. Flow rates were set at 5654.87 µL/min for the 5 mL syringe and 1413.72 µL/min for the 1 mL syringe. Eight deliveries were performed for each step, with a 10-second pause between the execution of G-codes. Additionally, a 1-milliliter glass syringe with a 6-millimeter inner diameter was used to dispense 1 millimeter of water, resulting in a 0.028-gram addition for each step.

Table 6. Random errors validating analytical performance of the pump.

Distance (mm)	Measured weight average gain (g)	Random error (g)	Random error (µL)
1	0.1175	0.0066	6.6
0.5	0.0575	0.0066	6.6
0.3	0.0325	0.0082	8.2
0.2	0.0228	0.0045	4.5
0.1 x 5	0.0385	0.0063	6.3
1 (1 mL syringe)	0.0274	0.0014	1.4

The results consistently showed that random errors remained below 10 microliters for each increment, highlighting the precision of our pump. As the targeted volume increased, the ratio of random error to target volume decreased. For dosage weights exceeding 0.05 grams, the random error remained consistent. This observation is understandable, considering the laboratory scale's sensitivity of 0.01 grams. It is also worth noting that random errors may result from flow path imperfections, such as pre-existing air bubbles in the syringe and unwanted frictions in the syringe's plunger. Moreover, due to the cohesive properties of water, siphoning and capillary effects may occur when handling small microliter volumes, potentially hindering the precise delivery of liquids.

3.2 Cost Analysis and Literature Comparison

In Table 7, both the overall cost and the expenses related to individual components are presented. Without electronic control, power system, and the syringe, the total cost of the pump is estimated at $20. It is noteworthy that 3D-printed bearings, as an alternative to conventional metal bearings, will effectively fulfill their function, resulting in cost and weight reductions ($2). The remaining additive cost is also a maximum of $20, as any 12V 2A AC-DC power supply and a low-cost Arduino board along with the CNC shield are deemed sufficient. Additionally, by utilizing an existing standard FDM 3D printer's stepper motor pin and its user interface—such as the X-axis hub of the printer—there will be no additional cost. Also, generic PE syringes are also very affordable, priced at under $1.

Table 7. Cost list of the used components.

Name	*Cost ($)*
3D parts	5
Step motor (17HS4401S)	10
Pulleys (2GT-20T X 1, idler pulley X 1)	1
Bearings (608ZZ X 4)	2
GT2 belt (40 cm)	2
Syringe	1
Arduino UNO (clone), CNC shield (OEM), 12V power supply (OEM), connectors	20
Total for the pump mechanism only	20
Total	**<41**

In Table 8, we present a comparative analysis between our 3D-printed syringe pump and those documented in the literature. The focus is on the cost, the extent of the requirement for non-3D printed parts, and the weight excluding stepper and controller electronics. In one study, Samokshin designed a pump with 3 µL precision using Arduino and a 3D printer (Samokhin 2020). However, the design necessitated the inclusion of additional components (lead screw nut, lead screw, and guide rod), which increased the weight and cost of the pump. Rogosic et al. designed a low-cost, customizable 3D-printed pump notable for its scalability and compactness (Rogosic et al. 2022). However, the linear rail design necessitated the use of metal parts, impacting cost-effectiveness. García et al. designed a dual-channel syringe pump using 3D printing, but the design included metal linear transmitters and relied on a heavy stand, reducing its portability (Garcia et al. 2018). Gervasi et al. designed a highly compact and portable syringe pump using open-source hardware and 3D printing, significantly reducing the cost through their practical design (Gervasi et al. 2021). However, the use of threaded rods in the linear rail system introduces limitations: it slightly increases both cost and weight, and as highlighted by Gervasi et al., introduces backlash problems that could affect precision.

Table 8. Comparative analysis with literature.

Reference	Cost	Not 3D printed parts	Weight
Our study.	18 or 20$	Screws-nuts, metal bearings (optional), pulleys	<250g
(Samokhin, 2020).	50 or 100	Metal bearings, lead screw and guide rods, screw-nuts, flanged round lead screw nut.	>500g
(Rogosic et al., 2022).	100 €	Metal bearings, lead screw and guide rods, flanged round lead screw nut, screw-nuts.	>500g
(Garcia et al., 2018).	>100$	Metal bearings, lead screw and guide rods, screw-nuts, flanged round lead screw nut.	>500g
(Cubberley & Hess, 2017).	60$	Lead screw, screw-nuts, flanged round lead screw nut.	>500g
(Gervasi et al., 2021).	50$	Lead screw, screw-nuts, flanged round lead screw nut.	>250g
(Baas & Saggiomo, 2021).	30 €	A complete 3D printer is required.	
(Ağır, 2023).	2$	A complete 3D printer is required.	<50g

Studies have shown that incorporating more non-3D-printed parts increases both cost and overall weight (Table 8). Our pump is distinguished by its reduced weight, a higher prevalence of 3D-printed components in contrast to traditional metal counterparts, and a lower overall cost. Also, several studies have described 3D-printed syringe pumps offering significant advantages in terms of cost and weight (Baas and Saggiomo 2021, Ağır 2023). However, these designs necessitate a functional 3D printer and lack standalone operation capabilities.

Additionally, in our experiments, to achieve lower costs and weight, we printed all 3D parts at 50% infill without compromising the mechanical stability and function of the pump, resulting in a 9% reduction in filament weight (first value of the range given in the table).

4. Conclusion

We presented a low-cost 3D-printed syringe pump, which offers versatility and practical utility in laboratory and research settings. In applications where the angle with respect to gravity may change, a standard lead screw often experiences varying backlash. Our choice of the belt drive over the lead screw effectively eliminated backlash issues. In this manner, we have also enabled unrestricted and real time rotation of the syringe pump in three dimensions. By implementing a 3D-printed linear rail with a belt drive mechanism, we successfully reduced the cost of a standalone 3D-printed syringe pump to $20 USD and its weight to 225 grams (excluding stepper and controller electronics). This pump design holds promise for enabling local production of 3D-printed syringe pumps, particularly in resource-scarce settings, thus enhancing their accessibility and usability in these regions. The described cost and weight, and as highlighted by Gervasi et al., introduces backlash problems that could affect precision. 3D syringe pump offers numerous potential applications within the biomedical and biotechnology domains, including fluid control in bioreactor setups, flow injection systems, tissue engineering, and drug delivery.

Declaration of Ethical Standards
The authors declare that they comply with all ethical standards.

Credit Authorship Contribution Statement
Author: Conceptualization, investigation, methodology and software, visualization and writing – original draft, funding acquisition

Declaration of Competing Interest
The authors have no conflicts of interest to declare regarding the content of this article.

Data Availability Statement
All data generated or analyzed during this study are included in this published article. (Datasets are available on request. The raw data supporting the conclusions of this article will be made available by the authors, without undue reservation). 3D models can be accessed on our online repository at http://github.com/ismailagir/BD3DSP.

5. References

Ağır İ., 2023. *Using the 3D printer as a programmable syringe pump.* The ICASEM 4th International Applied Sciences, Engineering, and Mathematics Congress. Tekirdağ, Türkiye, 215–223.

Baas S., Saggiomo V., 2021. Ender3 3D printer kit transformed into open, programmable syringe pump set. *HardwareX*, **10**, e00219. https://doi.org/10.1016/j.ohx.2021.e00219

Barik BB, Mahanty A, Majumder SD, Roy Goswami A., 2023. Fabrication of Cost-effective Three-axis portable mini-CNC milling Machine. *Mater Today: Proceedings.* (Article in press) https://dx.doi.org/10.1016/j.matpr.2023.03.012

Beaman JJ, Bourell DL, Seepersad CC, Kovar D., 2020. Additive Manufacturing Review: Early Past to Current Practice. *Journal of Manufacturing Science and Engineering, Transactions of the ASME*, **142(11)**, 110812-20.

https://dx.doi.org/10.1115/1.4048193

Bolat Ç., Ergene B., Ispartall H., 2023. A comparative analysis of the effect of post-production treatments and layer thickness on tensile and impact properties of additively manufactured polymers. *International Polymer Processing***, 38(2)**, 244-256. https://dx.doi.org/10.1515/ipp-2022-4267

Booeshaghi AS, Beltrame E da V, Bannon D, Gehring J, Pachter L., 2019. Principles of open-source bioinstrumentation applied to the poseidon syringe pump system. *Scientific Reports*, **9(1)**:1–8. https://dx.doi.org/10.1038/s41598-019-48815-9

Cubberley MS, Hess WA., 2017. An inexpensive programmable dual-syringe pump for the chemistry laboratory. *J Chem Educ,* **94(1)**:72–74. https://dx.doi.org/10.1021/acs.jchemed.6b00598

Darling C., Smith DA., 2021. Syringe pump extruder and curing system for 3D printing of photopolymers. *HardwareX*, **9**: e00175. https://dx.doi.org/10.1016/j.ohx.2021.e00175

Ergene B., 2022. Simulation of the production of Inconel 718 and Ti6Al4V biomedical parts with different relative densities by selective laser melting (SLM) method. *Journal of the Faculty of Engineering and Architecture of Gazi University*, **37 (1)**, 469 - 484 https://dx.doi.org/10.17341/GAZIMMFD.934143

Ergene B., Atlıhan G., Pinar AM., 2023. Experimental and finite element analyses on the vibration behavior of 3D-printed PET-G tapered beams with fused filament fabrication. *Multidiscipline Modeling in Materials and Structures,* **19(4)**, 634-651. https://dx.doi.org/10.1108/MMMS-11-2022-0265

Ergene B., Bolat Ç., 2022. An experimental investigation on the effect of test speed on the tensile properties of the PETG produced by additive manufacturing. *International Journal of 3D Printing Technologies and Digital Industry*, **6(2),** 250-260. https://dx.doi.org/10.46519/ij3dptdi.1069544

Garcia VE, Liu J, DeRisi JL., 2018. Low-cost touchscreen driven programmable dual syringe pump for life science applications. *HardwareX*, **4**, e00027. https://dx.doi.org/10.1016/j.ohx.2018.e00027

Gervasi A., Cardol P., Meyer PE., 2021. Open-hardware wireless controller and 3D-printed pumps for efficient liquid manipulation. *HardwareX*, **9**, e00199. https://dx.doi.org/10.1016/j.ohx.2021.e00199

Gucluer S., 2023. A Miniaturized Archimedean Screw Pump for High-Viscosity Fluid Pumping in Microfluidics. *Micromachines*, **14(7)**:1409 https://dx.doi.org/10.3390/mi14071409

Juarez A, Maynard K, Skerrett E, Molyneux E, Richards-Kortum R, Dube Q, Maria Oden Z., 2016. AutoSyP: A Low-Cost, Low-Power Syringe Pump for Use in Low-Resource Settings. *Am J Trop Med Hyg*., **95(4)**, 964-969. https://dx.doi.org/10.4269/ajtmh.16-0285

Kashaninejad N, Nguyen NT., 2023. Microfluidic solutions for biofluids handling in on-skin wearable systems. *Lab Chip*, **23(5)**, 913–937. https://dx.doi.org/10.1039/d2lc00993e

Khalid MS, Jaleed SM, Zafar A, Khan SA, Ur Rehman HZ, Khan ZH., 2023. *Design and Experimental Verification of a Laser Engraving Machine.* 2023 International Conference on Emerging Power Technologies. Topi, Pakistan, 1-6. https://doi.org/10.1109/ICEPT58859.2023.10152428

Klar V, Pearce JM, Kärki P, Kuosmanen P., 2019. Ystruder: Open source multifunction extruder with sensing and monitoring capabilities. *HardwareX*, **6**, e00080. https://dx.doi.org/10.1016/j.ohx.2019.e00080

Kukla M, Tarkowski P, Malujda I, Talaśka K, Górecki J., 2016. Determination of the torque characteristics of a stepper motor. *Procedia Engineering,* **136**, 375-379. https://dx.doi.org/10.1016/j.proeng.2016.01.226

Lake JR, Heyde KC, Ruder WC., 2017. Low-cost feedback-controlled syringe pressure pumps for microfluidics applications. *PLoS One*, **12(4)**, e0175089-12. https://doi.org/10.1371/journal.pone.0175089

Leuthner, M., & Hayden, O., 2024. Grease the gears: how lubrication of syringe pumps impacts microfluidic flow precision. *Lab on a Chip*, **24(1)**, 56-62. https://doi.org/10.1039/D3LC00698K

Liu DS, Lin PC, Lin JJ, Wang CR, Shiau TN., 2019. Effect of environmental temperature on dynamic behavior of an adjustable preload double-nut ball screw. *International Journal of Advanced Manufacturing Technology*, **101**, 2761–2770. https://dx.doi.org/10.1007/s00170-018-2966-x

Luo W, Liu G, Wang H., 2022. Study on Anti-backlash Mechanism Used in Precise Transmission: A Review. *Mechanisms and Machine Science.* **111**, 449–1470. https://dx.doi.org/10.1007/978-981-16-7381-8_89

Mapley M, Lu Y, Gregory SD, Pauls JP, Tansley G, Busch A., 2020. Development and validation of a low-cost polymer selective laser sintering machine. *HardwareX*, **8**. e00119. https://dx.doi.org/10.1016/j.ohx.2020.e00119

Ozer T, Agir I, Henry CS., 2022. Rapid prototyping of ion-selective electrodes using a low-cost 3D printed internet-of-things (IoT) controlled robot. *Talanta*, **247,** 123544-8. https://dx.doi.org/10.1016/j.talanta.2022.123544

Pusch K, Hinton TJ, Feinberg AW., 2018. Large volume syringe pump extruder for desktop 3D printers. *HardwareX*, **3**, 49–61. https://dx.doi.org/10.1016/j.ohx.2018.02.001

Rogosic R, Poloni M, Marroquin-Garcia R, Dimech D, Passariello Jansen J, Cleij TJ, Eersels K, van Grinsven B, Diliën H., 2022. Cost-effective, scalable and smartphone-controlled 3D-Printed syringe pump - From lab bench to point of care biosensing applications. *Physics in Medicine*, **14**, 100051-6 https://dx.doi.org/10.1016/j.phmed.2022.100051

Samokhin AS., 2020. Syringe Pump Created using 3D Printing Technology and Arduino Platform. *Journal of Analytical Chemistry*, **75(3)**, 416–421. https://dx.doi.org/10.1134/S1061934820030156

Schreiber DA, Richter F, Bilan A, Gavrilov P V., Man Lam H, Price CH, Carpenter KC, Yip MC., 2020. *ARCSnake: An Archimedes' Screw-Propelled, Reconfigurable Serpentine Robot for Complex Environments*. 2020 IEEE International Conference on Robotics and Automation (ICRA). Paris, France, 7029-7034. https://doi.org/10.1109/ICRA40945.2020.9196968

Shah J, Snider B, Clarke T, Kozutsky S, Lacki M, Hosseini A., 2019. Large-scale 3D printers for additive manufacturing: design considerations and challenges. International *Journal of Advanced Manufacturing Technology*. **104**, 3679–3693. https://doi.org/10.1007/s00170-019-04074-6

Tashman JW, Shiwarski DJ, Feinberg AW., 2022. Development of a high-performance open-source 3D bioprinter. *Scientific Reports,* **12**, 1–9. https://doi.org/10.1038/s41598-022-26809-4

Wang B, Si Y, Chadha C, Allison JT, Patterson AE., 2018. Nominal Stiffness of GT-2 Rubber-Fiberglass Timing Belts for Dynamic System Modeling and Design. *Robotics*, **7(4)**, 75. https://dx.doi.org/10.1038/s41598-022-26809-4

Wang Y, Li L, Ang WT, Gan L, Wang L, Huang F., 2023. Adaptive Backlash Compensation for CNC Machining Applications. *Machines*, **11**, 193-14. https://dx.doi.org/10.3390/machines11020193